Article published online: 2023-12-01

Solvents Influence ^{1}H NMR Chemical Shifts and Complete ^{1}H and ^{13}C NMR Spectral Assignments for Florfenicol

Wan-Ting Ai[1] Wei-Ke Su[1,2] Feng Su[1,2*]

[1] Collaborative Innovation Center of Yangtze River Delta Region Green Pharmaceuticals, Zhejiang University of Technology, Huzhou, People's Republic of China
[2] Zhejiang Governor Triangle Biomedical Industrial Technology Research Park, Zhejiang University of Technology, Huzhou, People's Republic of China

Address for correspondence Feng Su, PhD, College of Pharmaceutical Sciences, Zhejiang University of Technology, 18 Chaowang Road, Hangzhou 310014, People's Republic of China (e-mail: sufeng@zjut.edu.cn).

Pharmaceut Fronts 2023;5:e288–e296.

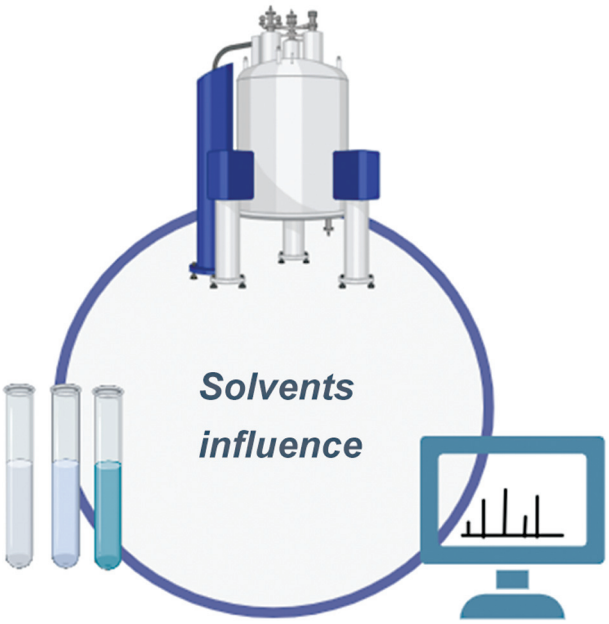

received
June 29, 2023
accepted
October 31, 2023
article published online
December 1, 2023

DOI https://doi.org/10.1055/s-0043-1777285.
ISSN 2628-5088.

Georg Thieme Verlag KG, Rüdigerstraße 14, 70469 Stuttgart, Germany

Abstract

Florfenicol (FFC) is an important and widely used veterinary drug, and its structure has been characterized by nuclear magnetic resonance (NMR) spectroscopy. The study aimed to investigate the influences of solvent type, solvent concentration, and temperature on the chemical shifts of the ^{1}H NMR of FFC. The results showed that different types of solvents significantly affected the chemical shifts, especially the chemical shifts of 2-H, 3-H, 5-H, and the active protons. When DMSO-d_6 is used as the solvent, there is no significant difference in the chemical shifts of FFC with a concentration ranging from 20 to 250 mmol/L; however, as the temperature increases, the chemical shifts of the active protons move to a higher field. Besides, the NMR spectroscopic data and structural analysis of FFC were refined by ^{1}H, ^{13}C, distortionless enhancement by polarization transfer-135 (DEPT-135), ^{1}H–^{1}H correlation spectroscopy (^{1}H–^{1}H COSY), phase-sensitive gradient heteronuclear singular quantum correlation (gHSQC), and heteronuclear multiple bond correlation (gHMBC) NMR spectroscopy using DMSO-d_6 as a solvent. The study will help with qualitative and quantitative analysis of FFC in the future.

Keywords

- florfenicol
- nuclear magnetic resonance
- solvents
- solvent concentrations
- chemical shifts

Introduction

Florfenicol (FFC) (►**Fig. 1**), a derivative of chloramphenicol, is an important broad-spectrum antibiotic that can diffusely enter into bacterial cells through fat solubility. FFC mainly acts on the 50s subunit of the bacterial 70s ribosome to inhibit peptidyl transferase and subsequent peptide chain elongation by blocking peptidase growth and peptide chain formation, thus, preventing the synthesis of bacterial proteins. FFC is frequently used to treat infectious infections in aquatic, livestock, and poultry, due to its advantages including potent antibacterial action, low risk of drug resistance, good absorption *in vivo*, high safety, high bioavailability, etc.[1–3] However, the growing use of FFC may be associated with adverse effects. Hassanin et al found that FFC-treated chickens had a significantly high number of adipocytes in the bone marrow, and the hematopoietic cell lines were moderately atrophied,[4] confirming the influence of FFC in hematopoietic and immune functions. Yun et al demonstrated a negative impact of oral administration of FFC on intestinal mucosal barriers, immune system, and intestinal microbiota.[5] Wang et al suggested a promoting effect of FFC on the oxidative stress response, which plays an important role in inducing kidney injury in broiler chickens.[6]

To protect food health and safety, the detection of FFC residue in animal and meat-derived foods has been gradually emphasized.[7–14] Chloramphenicol analogs usually have low residue levels in aquatic products, thus, it is necessary to use high sensitivity and low detection limit assays to detect them.

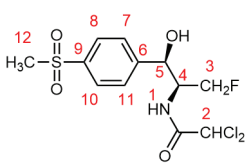

Fig. 1 Structure of FFC. FFC, florfenicol.

Li et al calculated the total residue levels of FFCs in eggs using an ultra-performance liquid chromatography-tandem mass spectrometry (UPLC-MS/MS) method to quantify the metabolite florfenicolamide.[15] Wang et al established a simple, rapid, and novel ultra-performance liquid chromatography with fluorescence detection (UPLC-FLD) method to determine methylsulfonamides, FFC, and its metabolite florfenicolamide residues in poultry eggs.[16] Patyra and Kwiatek used a liquid chromatography and diode array detector to simultaneously determine FFC and methylsulfonamides in medicinal feed.[17]

Nuclear magnetic resonance (NMR) is characterized by its speed and ease of use. NMR uses the relationship between the number of protons of a specific group in the molecule and the corresponding spectral peaks to quickly, accurately, and quantitatively analyze the components without the aid of the standards. With the advancement of NMR techniques in terms of hardware and software, quantitative analysis using NMR techniques has been paid increasing attention and has been used to study the changes in drugs in solvents.[18–25] In this study, the NMR technique was used to analyze the spectral data and the structure of FFC. Besides, the effects of solvents, FFC concentration, and temperature on the chemical shifts of the FFC ^{1}H NMR spectra were assessed. All ^{1}H and ^{13}C NMR chemical shifts were determined by advanced one-dimensional (1D) and two-dimensional (2D) NMR.

Experimental

Materials and Reagents

FFC used for spectral measurement was supplied by Zhejiang Hisoar Pharmaceutical Co. Ltd. (Taizhou, Zhejiang) with a purity of 99%. Chloroform-*d* ($CDCl_3$, 99.9 atom% D), acetonitrile-d_3 (ACN-d_3, 99.8 atom% D), acetic acid-d_4 (CD_3COOD, 99.5 atom% D), methanol-d_4 (CD_3OD, 99.8 atom% D), acetone-d_6 (CD_3COCD_3, 99.9 atom% D), methyl sulfoxide-d_6 (DMSO-d_6, 99.9 atom% D), *N*,*N*-dimethylformamide-d_7 (DMF-d_7, 99.5 atom% D), and pyridine-d_5 (C_5D_5N, 99.5 atom% D) were

purchased from Cambridge Isotope Laboratories Inc.(Cambridge, United States).

Apparatus and Conditions

The advanced 1D and 2D NMR spectra were recorded at 303 K on a Varian Mercury-Plus 400 MHz spectrometer (Varian, United States) operating at frequencies of 400.13 and 100.62 MHz using 5 mm ID probe for ^{1}H/^{13}C, respectively. Tetramethylsilane (δ 0.00 ppm) and DMSO-d_6 (δ 39.50 ppm) were used as the reference for the measurement of ^{1}H and ^{13}C NMR chemical shifts. Eight solutions in different solvents ($CDCl_3$, ACN-d_3, CD_3COOD, CD_3OD, CD_3COCD_3, DMSO-d_6, DMF-d_7, C_5D_5N) with FFC concentrations at 50 mmol/L, six solutions (20, 50, 100, 150, 200, 250 mmol/L) in DMSO-d_6, and three solutions (20, 100, 250 mmol/L) in DMSO-d_6 at different temperatures (303, 308, 313, 318, 323, 328, 333, 338, 343 K) were prepared for investigating the influences of ^{1}H NMR chemical shifts of FFC. ^{1}H NMR spectra were recorded with acquisition times of 2.5 seconds using a 45-degree pulse and ^{13}C spectra were obtained with acquisition times of 1.2 seconds using a 30-degree pulse. The distortionless enhancement by polarization transfer (DEPT) spectrum was recorded using relaxation delay times of 2 seconds by using a shaped pulse for a 180-degree pulse on the f1 channel with a 135-degree read pulse to give CH, CH_3 positive, and CH_2 negative. The 2D NMR spectra were recorded with standard pulse sequences supplied with the TopSpin 3.6.5 spectrometer software (Bruker DESKTOP-G4TBOV8). The ^{1}H–^{1}H COSY spectrum was recorded using one transient per t_1 increment with relaxation delay times of 2 seconds, spectral widths of 4587.2 Hz, and acquisition times of 0.223 seconds in t_2 with 128 complex t_1 increments. The phase-sensitive gradient heteronuclear singular quantum correlation (gHSQC) spectrum was obtained with polarization transfer and refocusing delays optimized for $^{1}J_{CH} = 150$ Hz; four transients were recorded for each of 128 complex t_1 increments with relaxation delay times of 2 seconds, spectral widths of 4,587.2/17,094.0 Hz, and acquisition times of 0.223 seconds in t_2. The heteronuclear multiple bond correlation (gHMBC) spectrum was obtained with polarization transfer delays optimized for $^{1}J_{CH} = 150$ Hz, $^{n}J_{CH} = 6$ Hz; four transients were recorded for each of 400 complex t_1 increments with relaxation delay times of 2 seconds, spectral widths of 4,587.2/24,154.6 Hz, and acquisition times of 0.223 seconds in t_2. All 1D and 2D spectra were processed using Mestrelab's Mnova software, version 7.1.0-9185 (Santiago de Compostela, Spain).

Results and Discussion

The Influences of Solvents on ^{1}H NMR of FFC

FFC dissolved in different solvents was used to identify changes in chemical shifts in ^{1}H NMR spectra. Approximately 9 mg of FFC was dissolved in 500 µL different pure solvents

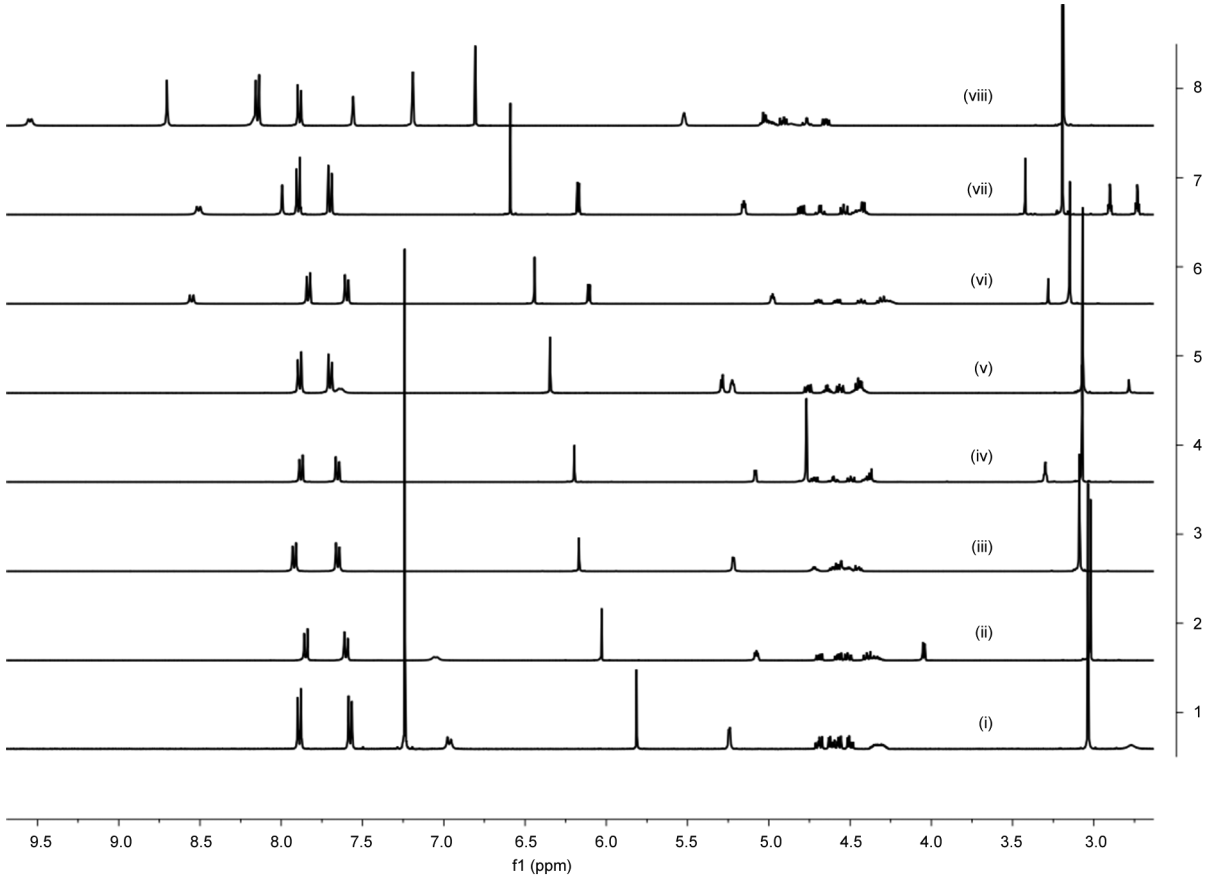

Fig. 2 ^{1}H NMR spectra of FFC at different solvents. (i)–(viii): $CDCl_3$, ACN-d_3, CD_3COOD, CD_3OD, CD_3COCD_3, DMSO-d_6, DMF-d_7, C_5D_5N, respectively; 400 MHz, temperature 303 K. FFC, florfenicol.

forming a concentration of 50 mmol/L, respectively, but the solubility of FFC in the $CDCl_3$ was very poor and saturated in the solution. Our data showed that the solvent causes a significant change in ^{1}H NMR chemical shifts (►**Fig. 2**). The entire elucidation of the hydrogen protons of the FFC in various solvents is displayed in ►**Table 1**. When CD_3OD and CD_3COOD were used, the active hydrogen protons disappeared due to the exchange with the deuterium hydrogen which made 5-H exhibit a doublet peak, while in other solvents (ACN-d_3, CD_3COCD_3, DMSO-d_6, DMF-d_7), the 5-H showed a doublet of doublet peak due to the coupling with both 4-H and the O–H. As a result, the O–H proton showed a double peak. The signals of O–H, 4-H, and 3-H were overlapping when using C_5D_5N as a solvent, which led to the difficulty of integration. Moreover, it was strange that the 5-H showed a single peak. The signals of 4-H and 3-H were overlapping when using CD_3COOD as a solvent, which made it difficult to determine the coupling constants. When $CDCl_3$ was used as a solvent, the signals of 4-H and 3-H were separated clearly. However, the coupling of 5-H with the O–H proton was not observed, which showed a doublet peak and a broad singlet peak, respectively. The N–H proton coupling with the 4-H was obvious. As far as 2-H was concerned, its chemical shift increased with the solvents' order as follows: $CDCl_3$, ACN-d_3, CD_3COOD, CD_3OD, CD_3COCD_3, DMSO-d_6, DMF-d_7, C_5D_5N, and the chemical shift moved to a low frequency from δ 5.81 to δ 6.81 ppm. All these results substantiate the solvent effect. The solvent effect mainly has the following aspects: firstly, different solvents have different solvent magnetic permeability, so FFCs are subjected to different magnetic field strengths, which affects the δ value. Secondly, the solvent molecules can be close to the solute molecules, which changes the electron cloud density of the solute molecules and produces a deshielding effect. In addition, the magnetic anisotropic effect of solvent molecules leads to shielding and deshielding effects on different parts of the solute molecules. Moreover, solvent molecules form hydrogen bonds with solute molecules, which can also affect the chemical shift of the hydrogen nucleus.[22,26] In particular, the aromatic solvent, C_5D_5N, showed the most pronounced changes.

The Influences of Solvent Concentrations on ^{1}H NMR of FFC

Generally, the concentration will also have a certain effect on the ^{1}H NMR chemical shift, acting mainly on changes in solution viscosity, changes in ion pairs, or changes in aggregation states.[27] In this work, six different concentrations of FFC solutions in DMSO-d_6 (20, 50, 100, 150, 200, 250 mmol/L) were used to further investigate the influence of concentrations on the ^{1}H NMR chemical shifts of FFC; however, no dramatical changes were found (►**Fig. 3**).

The Influences of Temperatures on ^{1}H NMR of FFC

To evaluate the influences of temperature, three solutions at different concentrations (20, 100, 250 mmol/L) of FFC in DMSO-d_6 were prepared for further experiments. The results showed that the samples with different concentrations at different temperatures exhibited similar changes in chemical shifts of active protons. The chemical shift of the O–H proton moved to a high frequency from δ 8.56 to δ 8.32 ppm when the temperature rose from 303 to 343 K. Every 5-degree temperature increase led to a 0.03 ppm chemical shift to the high frequency at the same time, the chemical shift of the N–H proton moved to a high frequency from δ 6.12 to δ 5.95 ppm, with 0.02 ppm of the chemical shift moving to the high field as the temperature increased 5 degrees. At high temperatures the thermal motion of the molecule is intensified, the degree of hydrogen bonding is reduced, and the density of the electron cloud around the hydrogen nucleus is increased making the hydrogen protons move into the higher field, and hence the corresponding chemical shift is reduced. The above changes were only found in active protons, while the chemical shifts of other protons did not significantly exhibit such changes. It was confirmed that the influence of temperature on active protons of FFC was greater than other protons (►**Fig. 4**).

The Structure Elucidation of FFC by Comprehensive NMR Analysis

The structure of FFC was elucidated with DMSO-d_6 as a solvent. Assignments of all ^{1}H NMR chemical shifts are summarized in ►**Table 2**. Hydrogen and carbon atoms were assigned by using ^{1}H NMR, full decoupling ^{13}C NMR, DEPT-135, ^{1}H–^{1}H COSY, gHSQC, and gHMBC. Among 14 hydrogen proton signals in the ^{1}H NMR spectrum, two active hydrogen protons were found with ^{1}H NMR chemical shifts at δ 6.15 ppm (O–H) and δ 8.62 ppm (N–H). Due to proton exchange, these two active hydrogen protons disappeared with a little D_2O added. The obtained signals in the range of δ 4.26 to 4.47 and δ 4.58 to 4.73 ppm corresponding to 3-H and 4-H respectively were multiplets, which seems inconsistent with the general split law due to the fluorine atom coupling with 3-H and 4-H. The 5-H (δ 5.00 ppm) signals were doublet of doublet due to the coupling with 4-H and O–H, which changed into a double signal when the hydrogen–deuterium exchanged. The 2-H was in a lower frequency (δ 6.45 ppm) compared with 4-H due to the deshielding effect of chlorine atoms and oxygen atoms. The 7-H and 11-H are chemically equivalent and have the same chemical shift (δ 7.61 ppm). The 8-H and 10-H are chemically equivalent as well (δ 7.85 ppm).

The ^{13}C NMR spectrum elucidation is shown in ►**Table 3**. There were 12 carbon signals shown in ^{13}C NMR in addition to the solvent peak, among which one primary carbon, six tertiary carbon, two secondary carbon, and three quaternary carbon atoms were found through the comparison among the DEPT-135 and full decoupling ^{13}C NMR. For the symmetry of the structure, the signal at δ 43.59 ppm in the highest frequency was assigned to 12-C and the signal at δ 163.41 ppm in the lowest frequency was assigned to the carbon in the carbonyl. The 3-C (δ 81.31, 83.00 ppm, $^1J_{CF}$ = 168.4), 4-C (δ 54.51, 54.71 ppm, $^2J_{CF}$ = 19.8), and 5-C (δ 69.28, 69.34 ppm, $^3J_{CF}$ = 5.7) exhibited a double peak due to the coupling with the fluorine atom by their coupling with 3-H, 4-H, and 5-H in gHSQC. The 2-C at δ 66.20 ppm was

Table 1 The ^{1}H NMR chemical shifts of FFC in different solvents

Solvent/ proton number	$CDCl_3$	ACN-d_3	CD_3COOD	CD_3OD	CD_3COCD_3	DMSO-d_6	DMF-d_7	C_5D_5N
2-H	5.81 (s)	6.03 (s)	6.17 (s)	6.20 (s)	6.35 (s)	6.44 (s)	6.59 (s)	6.81 (s)
3a′-H	4.48–4.52 (dd, 4.4, 9.2)	4.29–4.42 (m)	4.43–4.75 (m)	4.35–4.42 (m)	4.39–4.49 (m)	4.22–4.33 (m)	4.39–4.49 (m)	4.96–5.06 (m)
3a′′-H	4.56–4.63 (dd, 6.4, 9.2)	4.49–4.53 (dd, 6.8, 9.6)	4.43–4.75 (m)	4.47–4.51 (dd, 6.8, 9.2)	4.54–5.58 (dd, 6.4, 9.2)	4.41–4.45 (dd, 7.2, 9.2)	4.52–4.56 (dd, 6.8, 8.8)	4.63–4.67 (dd, 6.4, 9.2)
3b′-H	4.56–4.63 (dd, 4.4, 9.6)	4.56–4.59 (dd, 5.6, 9.2)	4.43–4.75 (m)	4.58–4.63 (m)	4.62–4.67 (m)	4.56–4.60 (dd, 5.2, 8.8)	4.66–4.71 (m)	4.74–4.79 (m)
3b′′-H	4.67–4.71 (dd, 6.8, 9.6)	4.67–4.71 (dd, 6.0, 9.6)	4.43–4.75 (m)	4.70–4.74 (dd, 6.0, 9.2)	4.74–4.78 (dd, 6.0, 9.2)	4.68–4.71 (dd, 5.2, 8.8)	4.78–4.82 (dd, 5.6, 9.2)	4.89–4.93 (dd, 6.4, 9.2)
4-H	4.27–4.37 (m)	4.29–4.42 (m)	4.43–4.75 (m)	4.35–4.42 (m)	4.39–4.49 (m)	4.22–4.33 (m)	4.39–4.49 (m)	4.96–5.06 (m)
5-H	5.24 (d, 2.8)	5.08 (dd, 4.0, 7.6)	5.22 (d, 3.2)	5.08 (d, 3.2)	5.22 (dd, 4.0, 7.2)	4.98 (dd, 4.0, 7.6)	5.16 (dd, 4.4, 7.6)	5.52 (s)
7-H 11-H	7.58 (d, 8.4)	7.60 (d, 8.4)	7.65 (d, 8.4)	7.65 (d, 8.4)	7.70 (d, 8.4)	7.60 (d, 8.4)	7.70 (d, 8.0)	7.89 (d, 8.0)
8-H 10-H	7.89 (d, 8.4)	7.85 (d, 8.4)	7.92 (d, 8.4)	7.88 (d, 8.4)	7.89 (d, 8.4)	7.83 (d, 8.4)	7.90 (d, 8.4)	8.15 (d, 8.4)
12-H	3.04 (s)	3.02 (s)	3.09 (s)	3.07 (s)	3.07 (s)	3.15 (s)	3.19 (s)	3.19 (s)
NH	6.97 (d, 8.4)	7.05 (d, 8.0)	–	–	7.64 (d, 6.8)	8.55 (d, 8.8)	8.51 (d, 8.4)	9.55 (d, 8.0)
OH	2.77 (s)	4.05 (d, 4.8)	–	–	5.29 (d, 4.4)	6.11 (d, 4.4)	6.17 (d, 4.4)	4.86 (br)

Abbreviation: FFC, florfenicol.

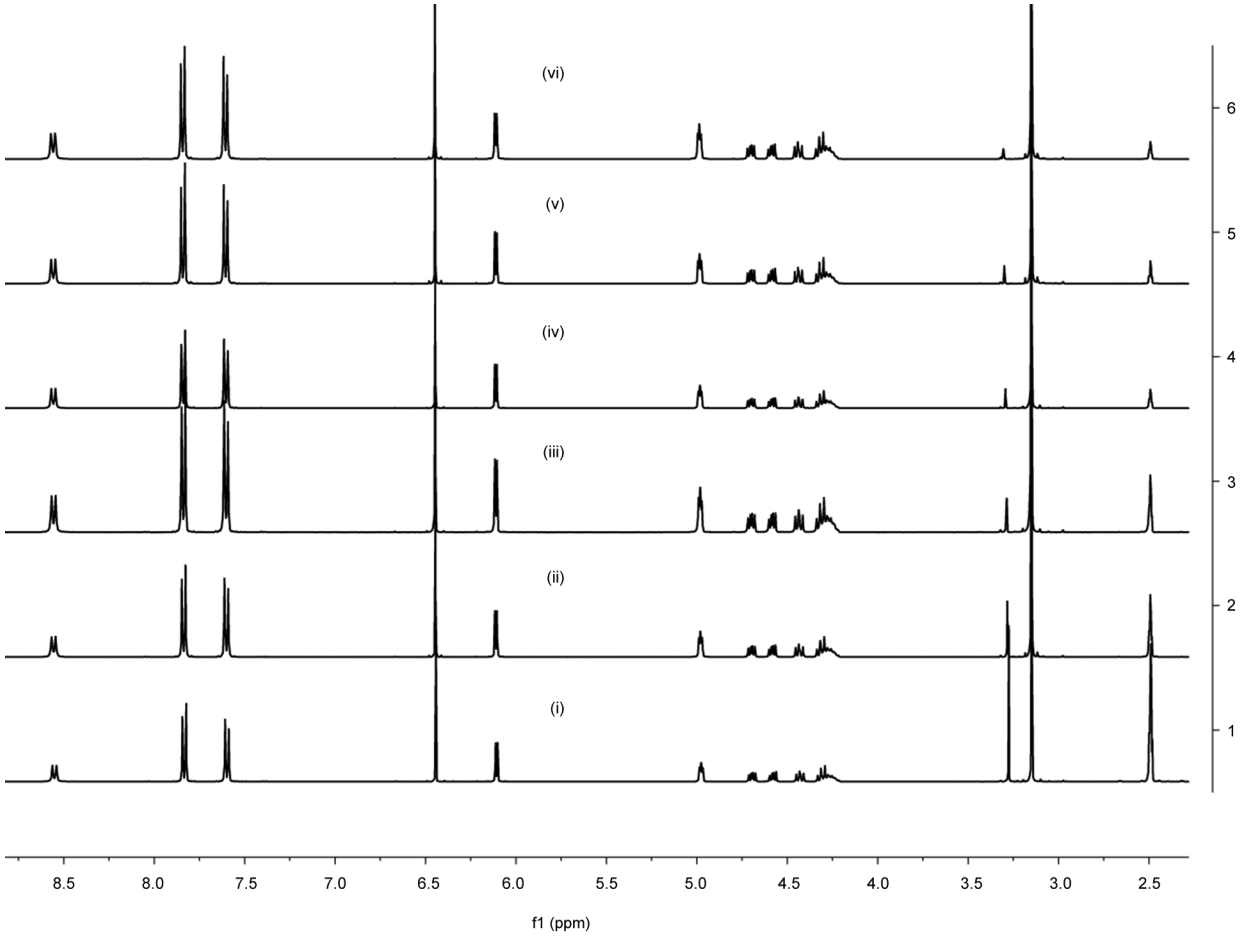

Fig. 3 ^{1}H NMR spectra of FFC at different concentrations in DMSO-d_6 solvent. (i)–(vi): 20, 50, 100, 150, 200, 250 mmol/L respectively; 400 MHz, temperature 303 K. FFC, florfenicol.

in a lower frequency compared with 4-C due to the deshielding effect of chlorine atoms and oxygen atoms. The signal at δ 126.26 ppm was assigned to 8-C and 10-C, and the 7-C and 11-C had the same chemical shift in the δ 126.92 ppm. The 9-C at δ 139.32 ppm could be confirmed by its coupling with 12-H in gHMBC. The signal at δ 147.61 ppm was assigned to 6-C by its coupling with 5-H in gHMBC.

Conclusion

In this study, we elucidated the structure of FFC and demonstrated that different types of solvents made obvious changes in their chemical shifts, especially on 2-H, 3-H, 5-H, and active protons. The clearer ^{1}H NMR spectrum was obtained when using $CDCl_3$ as the solvent, but the poor solubility of FFC in it made it difficult to obtain its ^{13}C NMR and 2D spectra. This is due to the molecular structure of FFC containing several polar groups, such as amide bond, –Cl, and –F, which have strong polarity, so it is difficult to dissolve in the weak polar solvent of $CDCl_3$. Therefore, DMSO-d_6 was eventually used for all the NMR spectra. Different concentrations of FFC in DMSO-d_6 at different temperatures were used to further evaluate the changes of ^{1}H NMR chemical shifts and no significant effects were found except for the active protons. As the temperature increases, the chemical shift of active protons gradually decreases because –OH and –NH form hydrogen bonds to a lesser extent at higher temperatures, and the chemical shift is shifted to a higher field. This investigation provided reasonable reference data for further research, especially the choice of the appropriate solvent and temperature, which can lead to significant changes in the ^{1}H NMR chemical shifts, signal separation, and spin–spin coupling constants.

NMR technology has the advantages of no damage, continuity, high resolution, and strong selectivity, and plays a significant role in compound structure identification, content detection, and dynamic tracking of the chemical reaction process. In future development, NMR can be combined with other analytical equipment, for digital intelligence, and more widely used in various fields.

Funding

The study is supported by the Zhejiang Science and Technology Plan Project (Grant No. 2021C03161), the Zhejiang Provincial Key R&D Project (Grant No. 2020C03006 & 2019-ZJ-JS-03), and the Natural Science Foundation of Zhejiang Province, China (Grant No. LQ18B050003).

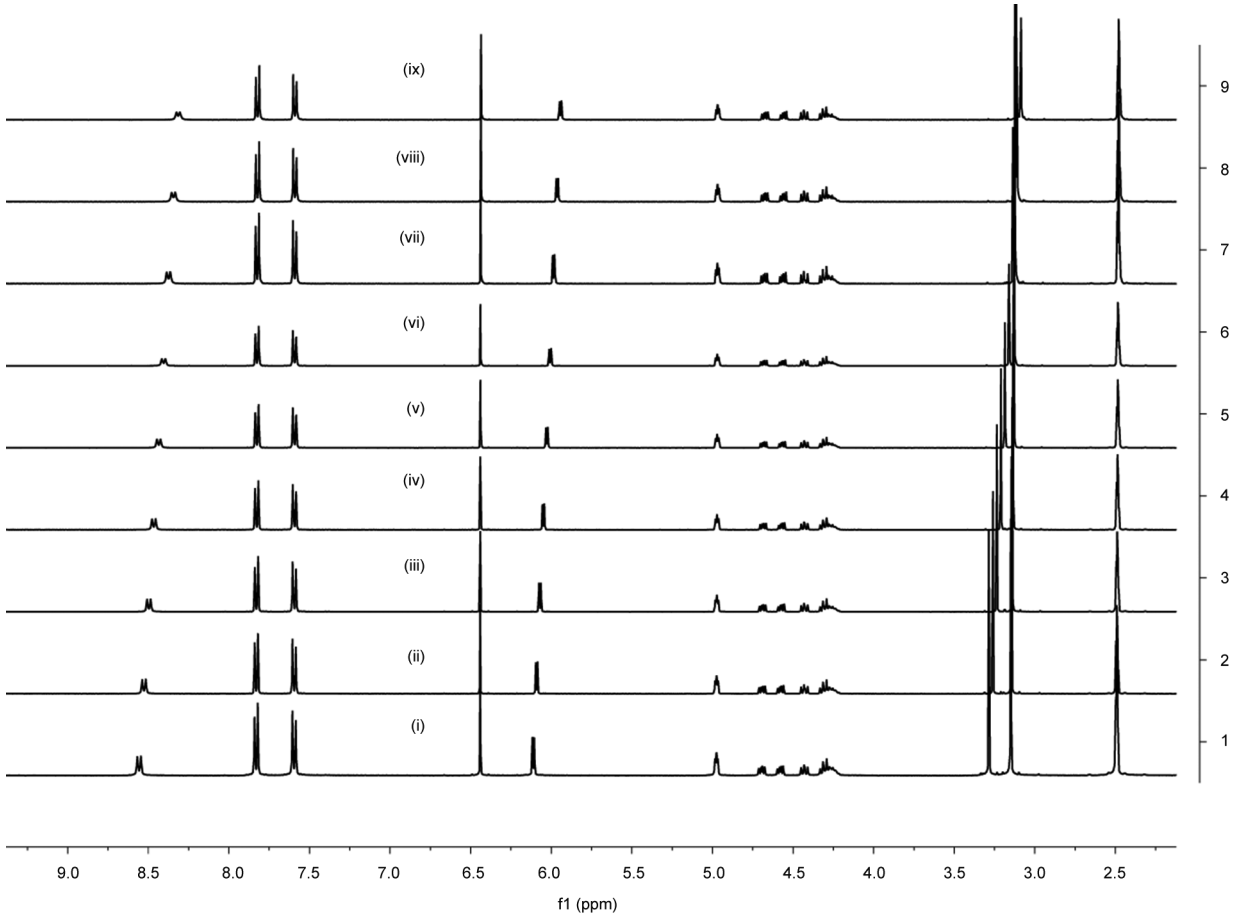

Fig. 4 ^{1}H NMR spectra of FFC at different temperatures in DMSO-d_6 solvent. (i) – (ix): 303, 308, 313, 318, 323, 328, 333, 338, 343, respectively; 400 MHz, 20 mmol/L. FFC, florfenicol.

Table 2 The ^{1}H NMR and ^{1}H-^{1}H COSY data of FFC

^{1}H chemical shifts δ_H ($\times 10^{-6}$) ppm	Multiplicity	Proton number	Coupling constant (Hz)	Assignment	^{1}H-^{1}H COSY δ_H ($\times 10^{-6}$) ppm
3.15	s	3	–	12-H	–
4.26–4.47	m, dd	2	7.2, 9.2	4-H, 3a-H	4.58–4.73 5.00, 8.62
4.58–4.73	dd, dd	1	5.2, 8.8 5.2, 9.2	3b-H	4.26–4.47
5.00	dd	1	4.0, 7.6	5-H	4.26–4.47, 6.15
6.15	d	1	4.4	OH	5.00
6.45	s	1	–	2-H	–
7.61	d	2	8.0	7-H, 11-H	7.85
7.85	d	2	8.0	8-H, 10-H	7.61
8.62	d	1	8.8	NH	4.26–4.47

Abbreviation: FFC, florfenicol.

Table 3 The ^{13}C NMR, DEPT, HSQC, and HMBC data of FFC

^{13}C chemical shifts δ_C ($\times 10^{-6}$) ppm	Carbon type	Carbon number	Assignment	HSQC δ_H ($\times 10^{-6}$) ppm	HMBC δ_H ($\times 10^{-6}$) ppm
43.59	CH_3	1	12-C	3.15	–
54.51, 54.71	CH	1	4-C	4.26–4.47	4.26–4.47, 4.58–4.73, 6.15, 8.62
66.20	CH	1	2-C	6.45	–
69.28, 69.34	CH	1	5-C	5.00	4.26–4.47, 6.15, 7.61
81.31, 83.00	CH_2	1	3-C	4.26–4.47, 4.58–4.73	4.58–4.73, 4.26–4.47
126.26	CH	2	8-C, 10-C	7.85	7.61, 7.85
126.92	CH	2	7-C, 11-C	7.61	5.00, 7.61, 7.85
139.32	C	1	9-C	–	3.15, 7.61, 7.85
147.61	C	1	6-C	–	5.00, 6.15, 7.61, 7.85
163.41	C	1	1-C	–	4.26–4.47, 6.45, 8.62

Abbreviation: FFC, florfenicol.

Conflict of Interest
None declared.

References

1 Blickwede M, Schwarz S. Molecular analysis of florfenicol-resistant Escherichia coli isolates from pigs. J Antimicrob Chemother 2004;53(01):58–64
2 Liu Y, Fang Y, Chen Y, et al. Improving intestinal absorption and antibacterial effect of florfenicol via nanocrystallisation technology. J Microencapsul 2022;39(7–8):589–600
3 Fan G, Zhang L, Shen Y, et al. Comparative muscle irritation and pharmacokinetics of florfenicol-hydroxypropyl-β-cyclodextrin inclusion complex freeze-dried powder injection and florfenicol commercial injection in beagle dogs. Sci Rep 2019;9(01):16739
4 Hassanin O, Abdallah F, Awad A. Effects of florfenicol on the immune responses and the interferon-inducible genes in broiler chickens under the impact of E. coli infection. Vet Res Commun 2014;38(01):51–58
5 Yun S, Guo Y, Yang L, et al. Effects of oral florfenicol on intestinal structure, function and microbiota in mice. Arch Microbiol 2020; 202(01):161–169
6 Wang X, Han C, Cui Y, et al. Florfenicol induces renal toxicity in chicks by promoting oxidative stress and apoptosis. Environ Sci Pollut Res Int 2021;28(01):936–946
7 Feng JB, Ruan HT, Chen HG, et al. Pharmacokinetics of florfenicol in the orange-spotted grouper, epinephelus coioides, following oral administration in warm seawater. J World Aquacult Soc 2018; 49(06):1058–1067
8 Li W, Guo F, Jiang X, Li Y, Li X, Yu Z. Compound ammonium glycyrrhizin protects hepatocytes from injury induced by lipopolysaccharide/florfenicol through oxidative stress and a MAPK pathway. Comp Biochem Physiol C Toxicol Pharmacol 2019;225:108585
9 Ma RR, Zhan J, Fang WH, et al. Pharmacokinetics and tissue distribution of bronopol in grass carp, Ctenopharyngodon Idella, at 15 and 20°C. Aquacult Res 2020;51(02):648–654
10 Osman K, Zolnikov TR, Badr J, et al. Vancomycin and florfenicol resistant Enterococcus faecalis and Enterococcus faecium isolated from human urine in an Egyptian urban-rural community. Acta Trop 2020;201:105209
11 Qian MR, Wang QY, Yang H, et al. Diffusion-limited PBPK model for predicting pulmonary pharmacokinetics of florfenicol in pig. J Vet Pharmacol Ther 2017;40(06):e30–e38
12 Li L. Rapid determination of chloramphenicol, thiamphenicol, and florfenicol residues in aquatic products by UPLC-MS/MS method. China Food Safety Magazine 2022;363(34):67–70
13 Wang Y, Li X, Wang Y, Schwarz S, Shen J, Xia X. Intracellular accumulation of linezolid and florfenicol in OptrA-Producing Enterococcus faecalis and Staphylococcus aureus. Molecules 2018;23(12):3195
14 Yang F, Yang F, Wang GY, et al. Effects of water temperature on tissue depletion of florfenicol and its metabolite florfenicol amine in crucian carp (Carassius auratus gibelio) following multiple oral doses. Aquaculture 2020;515:734542
15 Li X, Zhang Y, Sun Q, et al. Determination of extractable and non-extractable florfenicol residues as florfenicol amine in eggs by UPLC-MS/MS. Food Addit Contam Part A Chem Anal Control Expo Risk Assess 2022;39(09):1512–1520
16 Wang B, Xie X, Zhao X, et al. Development of an accelerated solvent extraction-ultra-performance liquid chromatography-fluorescence detection method for quantitative analysis of thiamphenicol, florfenicol, and florfenicol amine in poultry eggs. Molecules 2019;24(09):1830
17 Patyra E, Kwiatek K. HPLC-DAD analysis of florfenicol and thiamphenicol in medicated feedingstuffs. Food Addit Contam Part A Chem Anal Control Expo Risk Assess 2019;36(08):1184–1190
18 Chashmniam S, Tafazzoli M. NMR investigation and theoretical calculations of the solvent effect on the conformation of valsartan. J Mol Struct 2017;1148:73–80
19 Ghiasi R. Exploration of solvent effects on the spectroscopic properties (Ir and C ^{13} NMR) in the $OsCl_3(CCH_2CMe_3)(PH_3)_2$ carbyne complex. J Struct Chem 2018;59(05):1052–1057
20 Kaştaş G, Albayrak Kaştaş Ç, Tabak A. Investigation of molecular structure and solvent/temperature effect on tautomerism in (E)-4,6-dibromo-3-methoxy-2-[(p-tolylimino)methyl]phenol, a new thermochromic Schiff base, by using XRD, FT-IR, UV-vis, NMR and DFT methods. Spectrochim Acta A Mol Biomol Spectrosc 2019; 222:117198
21 Kauch M, Pecul M. Spin-spin artificial DNA intercalated with silver cations: theoretical prediction. ChemPhysChem 2012;13 (05):1332–1338
22 Korac J, Todorovic N, Zakrzewska J, et al. The conformation of epinephrine in polar solvents: an NMR study. Struct Chem 2018; 29(05):1533–1541
23 Niwayama S, Hiraga Y, Chaki S. ^{13}C NMR spectroscopic studies for the behaviors of carbonyl compounds in various solvents. Tetrahedron Lett 2017;58(50):4677–4681

24 Patel AK, Mishra SK, Krishnamurthy K, Suryaprakash N. Retention of strong intramolecular hydrogen bonds in high polarity solvents in binaphthalene-benzamide derivatives: extensive NMR studies. RSC Advances 2019;9(56):32759–32770
25 de Melo Sousa CM, Giordani RB, de Almeida WAM, et al. Effect of the solvent on the conformation of monocrotaline as determined by isotropic and anisotropic NMR parameters. Magn Reson Chem 2021;59(05):561–568
26 Kim H, Babu CR, Burgess DJ. Quantification of protonation in organic solvents using solution NMR spectroscopy: implication in salt formation. Int J Pharm 2013;448(01):123–131
27 Xu L, Huang B, Hou Z, Huang S, Zhao Y. Solvent effects used for optimal simultaneous analysis of amino acids via ^{19}F NMR spectroscopy. Anal Chem 2023;95(05):3012–3018

